International Journal of Geomechanics. Submitted January 11, 2016; accepted June 27, 2016; doi:10.1061/ (ASCE)GM.1943-5622.0000774

Modeling Pile Setup in Natural Clay Deposit Considering Soil Anisotropy, Structure and Creep Effects: Case Study

Mohammad Rezania[1]; Mohaddeseh Mousavi Nezhad[2]; Hossein Zanganeh[3]; Jorge Castro[4]; and Nallathamby Sivasithamparam[5]

Abstract: In this paper the behavior of a natural soft clay deposit under the installation of a case study pile is numerically investigated. The case study problem includes installation of an instrumented close-ended displacement pile in a soft marine clay deposit in Scotland, known as Bothkennar clay. The site has been used for a number of years as a geotechnical test bed site and the clay has been comprehensively characterized with both in-situ tests and laboratory experiments. The soft soil behavior, both after pile installation and subsequent consolidation, is reproduced by using an advanced critical state-based constitutive model, namely S-CLAY1S, that accounts for the anisotropy of soil fabric and destructuration effects during plastic straining. Furthermore, a time-dependent extension of S-CLAY1S model, namely Creep-SCLAY1S is used to study soil creep and the significance of its consideration on examining the overall pile installation effects. The simulation results are compared against field measurements; furthermore, for comparison the pile installation is also analyzed using the well-known isotropic modified

[1] Assistant Professor in Geomechanics, Department of Civil Engineering, University of Nottingham, Nottingham, NG7 2RD, UK. (corresponding author). E-mail: mohammad.rezania@nottingham.ac.uk.
[2] Assistant Professor in Geotechnical Engineering, School of Engineering, University of Warwick, Coventry, CV4 7AL, UK. E-mail: m.mousavi-nezhad@warwick.ac.uk.
[3] Research Fellow, Nottingham Centre for Geomechanics, Department of Civil Engineering, University of Nottingham, Nottingham, NG7 2RD, UK. E-mail: hossein.zanganeh@nottingham.ac.uk.
[4] Lecturer, Department of Ground Engineering and Materials Science, University of Cantabria, Avda. de Los Castros, s/n, 39005 Santander, Spain. E-mail: castrogj@unican.es.
[5] Project Geotechnical Engineer, Computational Geomechanics Division, Norwegian Geotechnical Institute NO-0806 Oslo, Norway. E-mail: nallathamby.siva@ngi.no.

Cam-clay model to highlight the importance of considering inherent features of natural soil such as anisotropy and structure in the simulations. A series of sensitivity analysis is also performed to evaluate the influence of initial anisotropy and bonding values on simulation results and to check the reliability of the numerical analyses.

Introduction

Since piles have to carry design loads for long periods of time, the consequences of soil modification around the pile, caused by its installation, are of great importance to variations of pile capacity. This is of more concern for piles in clays as for them the end bearing usually contributes a little to the overall pile capacity; while skin friction along the shaft constitutes the major portion of the pile function especially when there is no reliable soil layer at the end point of the pile. Therefore, field and laboratory investigations of the effects of pile installation on the properties of natural clays have been the subject of a large number of research studies over the past few decades (e.g., Holtz and Lowitz 1965; Roy et al. 1981; O'Neill et al. 1982; Heydinger and O'Neill 1986; Azzouz and Morrison 1988; Bond and Jardine 1991; Collins and Stimpson 1994; Burns and Mayne 1999; Pestana et al. 2002; Gallagher et al. 2005). However, there are still considerable uncertainties involved in the prediction of the capacity and performance of frictional driven piles in clays (Niarchos 2012). Particularly the increase in the capacity of displacement piles with time in clayey deposits, that are subject to significant increase in pore pressure during pile setup, has been widely debated (e.g., Randolph et al. 1979; Kavvadas 1982; Konrad and Roy 1987; Fellenius et al. 1989; Svinkin et al. 1994; Clausen and Aas 2000; Augustesen et al. 2006; Liyanapathirana 2008; Gwizdała and Więcławski 2013). Reliable prediction of the installation effects of piles on the inherent properties of natural deposits in which they are installed is essential for accurate and efficient design of these CO2 heavy and relatively expensive geo-

International Journal of Geomechanics. Submitted January 11, 2016; accepted June 27, 2016; doi:10.1061/ (ASCE)GM.1943-5622.0000774

structures. However, in spite of a few recent efforts (e.g., Sheil et al. 2015), in most of the studies so far primarily simple analytical methods have been developed or employed to simulate changes of soil properties around the pile shaft during and after installation. This is in large part due to the lack of numerical models capable of simulating the influential features of natural soil behavior, such as anisotropy, inter-particle bonding (structure), degradation of bonds (destructuration), rate dependency and etc., at a practical scale.

The main objective of this study is to numerically analyze the effects of a single pile setup in a cohesive soil layer, by primarily evaluating the effective stress variations and pore pressure dissipations around the pile after installation and during subsequent equalization (i.e., dissipation of excess pore pressures). It is also aimed to illustrate the practical capabilities of advanced soil models for evaluating soil alteration due to pile driving and prediction of pile capacity with time from a numerical standpoint. Pile installation has been modeled as an undrained expansion of a cylindrical cavity in the soil medium, commonly known as cavity expansion method (CEM) (Soderberg 1962; Carter et al. 1979; Randolph et al. 1979; Yu 1990; Yu 2000). Although, CEM does not model the full pile jacking procedure, it has proven to be practically a more versatile approach for conducting parametric studies of both short-term and long-term pile installation effects (Castro et al. 2013; Sheil et al. 2015). The numerical analyses are conducted using an anisotropic critical state-based effective stress soil model and a new time-dependent creep constitutive model. The analysis of the soil-pile load transfer mechanism and the mechanical response in the pile structure are beyond the scope of this paper and hence are not addressed here.

Constitutive Models

It is a well-established fact that the yield curves obtained from experimental tests (with triaxial or hollow cylinder apparatuses) on undisturbed samples of natural clays are inclined due

to the inherent fabric anisotropy in the clay structure (Graham et al. 1983; Dafalias 1987; Wheeler et al. 1999; Nishimura et al. 2007). Since consideration of full anisotropy in modeling soil behavior is not practical, due to the number of parameters involved, efforts have been mainly focused on the development of models with reduced number of parameters while maintaining the capacity of the model (Kim 2004). In order to capture the effects of anisotropy on soil behavior, a number of researchers have proposed anisotropic elasto-plastic constitutive models involving an inclined yield curve that is either fixed (Sekiguchi and Ohta 1977; Zhou et al. 2005) or is able to rotate in order to simulate the development or erasure of anisotropy during plastic straining (Davies and Newson 1993; Whittle and Kavvadas 1994; Wheeler et al. 2003; Dafalias et al. 2006). Among the developed anisotropic models, S-CLAY1 model (Wheeler et al. 2003) has been successfully used on different applications and accepted as a pragmatic anisotropic model for soft natural clays (Karstunen et al. 2006, Yildiz 2009, Zwanenburg 2013). In this model the initial plastic anisotropy is considered to be cross-anisotropic, which is a realistic assumption for normally consolidated clays deposited along the direction of consolidation. The model accounts for the development or erasure of anisotropy if the subsequent loading produces irrecoverable strains, resulting in a generalized plastic anisotropy. For simplicity, in this model the elastic behavior is assumed to be isotropic, which is a realistic assumption given the developed model is intended for applications with normally consolidated or lightly overconsolidated soft clays where even a small amount of stress increment is likely to cause yielding (Wheeler et al. 2003). The main advantages of the S-CLAY1 model over other proposed models are i) relatively simple model formulation, ii) realistic K_0 prediction, and most importantly iii) model parameters can be determined from standard laboratory tests using well-defined methodologies (Karstunen et al. 2005). The model has been further developed to also take account of bonding and destructuration effects (Karstunen et al. 2005), and very recently, time effects (Sivasithamparam et al. 2015) as

additional important features of natural soils' behavior. In the following the basics of these two advanced extensions of S-CLAY1 model, employed in this study, are explained in further detail.

S-CLAY1S Model

S-CLAY1S (Karstunen et al. 2005) is an extension of S-CLAY1 model that, in addition to plastic anisotropy, accounts for inter-particle bonding and destructuration of bonds during plastic straining. In three-dimensional stress space the yield surface of the S-CLAY1S model forms a sheared ellipsoid (similar to S-CLAY1) that is defined as

$$f_y = \frac{3}{2}[\{\boldsymbol{\sigma_d} - p'\boldsymbol{\alpha_d}\}^T\{\boldsymbol{\sigma_d} - p'\boldsymbol{\alpha_d}\}] - \left[M^2 - \frac{3}{2}\{\boldsymbol{\alpha_d}\}^T\{\boldsymbol{\alpha_d}\}\right](p'_m - p')p' = 0 \quad (1)$$

In the above equation $\boldsymbol{\sigma_d}$ and $\boldsymbol{\alpha_d}$ are the deviatoric stress and the deviatoric fabric tensors respectively, M is the critical state value, p' is the mean effective stress, and p'_m is the size of the yield surface related to the soil's preconsolidation pressure (see Fig. 1). The effect of bonding in the S-CLAY1S model is described by an intrinsic yield surface (Gens and Nova 1993) that has the same shape and inclination of the natural yield surface but with a smaller size. The size of the intrinsic yield surface is specified by parameter p'_{mi}which is related to the size $p'_m$of the natural yield surface by parameter χ, the current amount of bonding

$$p'_m = (1 + \chi)p'_{mi} \quad (2)$$

S-CLAY1S model incorporates three hardening laws. The first of these is the isotropic hardening law similar to that of modified Cam-clay (MCC) model (Roscoe and Burland 1968) that controls the expansion or contraction of the intrinsic yield surface as a function of plastic volumetric strain increments ($d\varepsilon_v^p$)

$$dp'_{mi} = \frac{vp'_{mi}}{\lambda_i - \kappa} d\varepsilon_v^p \quad (3)$$

where v is the specific volume, $\lambda_i$is the gradient of the intrinsic normal compression line in the compression plane ($\ln p' - v$ space), and κ is the slope of the swelling line in the compression plane. The second hardening law is the rotational hardening law, which describes the rotation of the yield surface with plastic straining (Wheeler et al. 2003)

$$d\boldsymbol{\alpha}_d = \omega \left[\left(\frac{3\boldsymbol{\eta}}{4} - \boldsymbol{\alpha}_d \right) \langle d\varepsilon_v^p \rangle + \omega_d \left(\frac{\boldsymbol{\eta}}{3} - \boldsymbol{\alpha}_d \right) \left| d\varepsilon_d^p \right| \right] \tag{4}$$

where $\boldsymbol{\eta}$ is the tensorial equivalent of the stress ratio defined as $\boldsymbol{\eta} = \boldsymbol{\sigma}_d / p'$, $d\varepsilon_d^p$ is the increment of plastic deviatoric strain, and ω and ω_d are additional soil constants that control the absolute rate of the rotation of the yield surface toward its current target value, and the relative effectiveness of plastic deviatoric strains and plastic volumetric strains in rotating the yield surface, respectively. The third hardening law in S-CLAY1S model is destructuration, which describes the degradation of bonding with plastic straining. The destructuration law (Karstunen et al. 2005) is formulated in such a way that both plastic volumetric strains and plastic shear strains tend to decrease the value of the bonding parameter χ towards a target value of zero which reads

$$d\chi = -\xi\chi\left(\left| d\varepsilon_v^p \right| + \xi_d \left| d\varepsilon_d^p \right| \right) \tag{5}$$

where ξ and ξ_d are additional soil constants. Parameter ξ controls the absolute rate of destructuration, and parameter $\xi_d$controls the relative effectiveness of plastic deviatoric strains and plastic volumetric strains in destroying the inter-particle bonding. The elastic behavior in the model is formulated with the same isotropic relationship as in the MCC model requiring the values of two parameters, κ and the Poisson's ratio, v' (to evaluate the value of elastic shear modulus, G').

Creep-SCLAY1S Model

The Creep-SCLAY1 model (Sivasithamparam et al. 2015) is an extension of S-CLAY1 to account for time-dependent response of clays. In this model the elliptical surface of the S-CLAY1 model is adopted as the normal consolidation surface (NCS) that is the boundary between small and large irreversible (creep) strains. Furthermore, in this model creep is formulated using the concept of a constant rate of visco-plastic multiplier (Grimstad et al. 2010) as

$$\dot{\Lambda} = \frac{\mu^*}{\tau}\left(\frac{p'_{eq}}{p'_p}\right)^{\beta}\left(\frac{M^2-\alpha^2_{K_0^{nc}}}{M^2-\eta^2_{K_0^{nc}}}\right) \tag{6}$$

where p'_p is the size of the outer rotated ellipse (see Fig. 2) which defines the NCS, p'_{eq} is the size of the current stress surface (CSS) that is the inner ellipse passing through the current state of effective stress, μ^* is the modified creep index, τ is a reference time that is set to 1 day if the NCS is derived from a standard oedometer test (see Leoni et al. 2008 for details), $\alpha_{K_0^{nc}}$ defines the inclinations of the ellipses in normally consolidated state (assuming K_0 consolidation history), $\eta^2_{K_0^{nc}} = 3(1-K_0^{nc})/(1+2\,K_0^{nc})$, and the additional term $(M^2-\alpha^2_{K_0^{nc}})/(M^2-\eta^2_{K_0^{nc}})$ is added to ensure that under oedometeric conditions the resulting creep strain corresponds to the measured volumetric creep strain rate (Sivasithamparam et al. 2015). Moreover, β is defined as $\beta = (\lambda^*-\kappa^*)/\mu^*$ where λ^* and κ^* are the modified compression and swelling indices, respectively, and μ^* is related to the one-dimensional secondary compression index C_α and the initial void ratio e_0 as $\mu^* = C_\alpha/[\ln 10\,(1+e_0)]$.

The size of NCS evolves with volumetric creep strains ε_v^c according to the following isotropic hardening law

$$p'_p = p'_{p0}exp\left(\frac{\varepsilon_v^c}{\lambda^*-\kappa^*}\right) \tag{7}$$

where p'_{p0} is the initial effective preconsolidation pressure. Adopting the same function as that of the NCS, the size of the CSS is obtained from the current stress state (p' and q) using the intersection of the vertical tangent to the ellipse with the p' axis as

$$p'_{eq} = p' + \frac{3}{2}\frac{\lfloor\{\boldsymbol{\sigma_d} - p'\boldsymbol{\alpha_d}\}^T\{\boldsymbol{\sigma_d} - p'\boldsymbol{\alpha_d}\}\rfloor}{\left[M^2 - \frac{3}{2}\{\boldsymbol{\alpha_d}\}^T\{\boldsymbol{\alpha_d}\}\right]p'} \tag{8}$$

where p'_{eq} is also known as the equivalent mean effective stress. The Creep-SCLAY1 model incorporates the same rotational hardening law as S-CLAY1 and S-CLAY1S models. Recently, the Creep-SCLAY1 model has been further extended to take into account the soil structure by adopting the destructuration hardening law of the S-CLAY1S model, as described in the previous section. The new extended model is called Creep-SCLAY1S.

Case Study

Bothkennar clay is a normally consolidated to slightly overconsolidated marine clay deposited on the southern bank of the Forth River Estuary near Stirling, located approximately midway between Glasgow and Edinburgh in Scotland. Bothkennar was an Engineering and Physical Science Research Council's geotechnical test site for which a comprehensive series of tests was performed in the early 90s to evaluate the properties of the high plasticity silty clay at the site. The resulting test data were reported and are available in the collection of papers in *Géotechnique Symposium-in-Print* (Vol. 42, No. 2, 1992). Since then it has also been the subject of a number of more advanced experimental investigations (e.g., Albert et al. 2003, Houlsby et al. 2005, McGinty 2006). Lehane and Jardine (1994) conducted a series of field experiments using high quality instrumented piles developed at Imperial College. The displacement piles employed in the investigation were equipped to measure pore pressures and effective stresses acting on the

soil-pile interface during pile installation and following consolidation. Two different pile lengths of 3.2m and 6m were studied, and the diameter of the case study piles was uniformly 102mm. From the base of a 1.2m deep cased hole, the cone-ended steel tubular piles were jacked into the ground at a rate of 500mm per minute in a series of 200mm pushes that were separated by pause periods of about 3 minutes. The general configuration of the 6m long model pile that has been selected for this study is shown in Fig. 3.

As shown in the figure different sensors to measure axial load, radial stress, shear stress and pore pressure were used at three clusters located along the lower 3m section of the pile, further details with regards to the instrumentation of the test piles can be found in Bond et al. (1991). Note that in the following the instruments are referred to by their distances from the pile tip (h) normalized by the pile radius (R) (see Fig. 3). The profile of the natural deposit penetrated by the instrumented piles can also be seen in Fig. 4, it includes a 1m deep overconsolidated dry crust followed by 5m deep layer of lightly overconsolidated Bothkennar clay with overconsolidation ratio (OCR) value of around 1.5.

Numerical Model and Simulations

The two advanced constitutive models described earlier in the paper have been implemented as user defined models in PLAXIS 2D AE version (Brinkgreve et al. 2013) using the fully implicit numerical solution proposed by Sivasithamparam (2012). Using each of the implemented models for the deformation calculations, PLAXIS carries out the coupled flow-deformation consolidation analysis based on Biot's theory.

The geometry of the numerical model for pile installation and the schematic sketch of different soil layers are shown in Fig. 5. As it is shown in the figure the groundwater table is located 1m below the ground surface. Taking advantage of the symmetry of the problem,

International Journal of Geomechanics. Submitted January 11, 2016; accepted June 27, 2016; doi:10.1061/ (ASCE)GM.1943-5622.0000774

axisymmetry condition is assumed in the finite element analysis. Parametric studies have been carried out to find out how wide the model should be to have a negligible influence of the outer boundary on the results. An extent of 3m from the symmetry axis in the horizontal direction was found to be sufficient. The depth of the model is selected to be the same as the length of the pile (i.e., 6m) in order to avoid modeling the pile tip, which can cause numerical instabilities. Roller boundaries are applied to all sides in order to enable the soil moving freely due to cavity expansion. Drained conditions and zero initial pore pressures are assumed above the water table. Also a drainage boundary is considered at the ground level and dynamic effects are ignored in the numerical model. A finite element mesh with 4048 15-noded triangular elements, resulting in 33021 nodes, is used in the analyses. Each element has pore water pressure degrees of freedom at corner nodes. Mesh sensitivity studies have been carried out to ensure that the mesh is dense enough to produce accurate results for both constitutive models. Towards the cavity wall much finer elements are used in order to provide better resolution in this zone with expected high strain gradients. The problem is modeled using large strain analyses with updated pore pressures, taking advantage of the updated Lagrangian formulation in PLAXIS.

Undrained pile installation is modeled as the expansion of a cylindrical cavity through development of a prescribed displacement from a small initial radius to a final, larger, radius (see Fig. 5). Similar to the pile, a cavity radius r_c of 0.05m has been selected, and a time interval of 0.1 day has been specified for the application of the prescribed displacement. There are other techniques for modeling the expansion of the cavity, e.g., applying an internal volumetric strain, however a prescribed displacement has been proven to be more practical particularly in terms of numerical stability (Kirsch 2006). As stated above, there is extensive laboratory data available for Bothkennar clay which makes it possible to derive a consistent set of material parameters for the advanced constitutive models used in this study. The initial values of state variables, as well as the values of conventional soil constants and additional model parameters are summarized in

Table 1. The initial state variables include the initial void ratio e_0, OCR, the initial degree of anisotropy α_0, and the initial amount of structure χ_0 (see Table 1). The conventional soil constants include unit weight γ, elastic constants (slope of the swelling line κ and Poisson's ratio ν'), and plastic constants (slopes of the normal compression line λ and the critical state line M). Based on the values of λ, κ and e_0, it is easy to calculate the corresponding values for the Creep-SCLAY1S model (λ^*=0.10 and κ^*=0.0067). In Table 1, the additional soil constants related to the evolution of anisotropy (ω and ω_d) and destructuration (ξ and ξ_d), are also listed together with the intrinsic compressibility λ_i. The latter needs to be used as the model parameter instead of λ for a natural soil, when the destructuration hardening law is used. The methodology for deriving these soil constants has been discussed by Leoni et al. (2008) and Sivasithamparam et al. (2015) and is not repeated here.

Table 2 lists the values for the viscosity parameters which are similar to the soft soil creep model (Vermeer et al. 1998), and the anisotropic creep model (Leoni et al. 2008). During the coupled consolidation analysis, the value of permeability coefficient k is assumed to be constant. The values for soil permeability (summarized in Table 3) are taken from literature (Géotechnique Symposium-in-Print 1992). In Table 3, k_v denotes vertical permeability obtained from tests on vertical soil samples and k_h denotes horizontal permeability obtained from tests on horizontal soil samples.

The behavior of the overconsolidated dry crust layer is modeled with a simple linear elastic-perfectly plastic Mohr-Coulomb model using the following relevant parameter values for the Bothkennar clay; E =3MPa, ν'=0.2, φ'=30°, ψ'=0°, c'=6kPa, and γ =19kN/m^{-3}. It should also be added that the initial state of stress is generated by adopting K_0-procedure (Brinkgreve et al. 2013). In addition to the two advanced models, S-CLAY1S and Creep-SCLAY1S, the boundary value problem is also modeled with the commonly used MCC

model in order to better highlight the advantages of considering natural features of soil behavior such as anisotropy, structure and time effects on reliability of the simulation results. The simulation results presented in the following sections are all based on model predictions at a point on the surface of the cavity and at the depth of $h/R = 28$ (the same depth as the depth of the middle cluster sensors on the pile surface).

Numerical Simulation Results

Total stress, pore pressure and effective stress variations

Fig. 6 shows the experimental measurements and numerical predictions of radial total stresses σ_{ri} during pile installation, at the pile surface. The field measurements in the figure were recorded by instruments at eight radii from the pile tip (i.e., at $h/R = 8$) and when the pile tip penetrated farther by instruments at $h/R = 28$. The figure illustrates that similar to the experimental results, the S-CLAY1S and Creep-SCLAY1S models predict the radial stresses, developed during pile jacking, to lie between the initial undisturbed horizontal stress σ_{h0} and the limit pressure. The limit pressure was measured through self-boring pressuremeter tests (Lehane and Jardine 1994). The figure also shows that the MCC model overestimates the radial total stresses and predicts them to exceed the pressuremeter limit pressure at depths beyond 3.5m.

The numerical predictions of Fig. 6, which are qualitatively consistent with the experimental results, indicate that the radial total stresses in Bothkennar clay increase with the increase of penetration depth. Such trend has also been observed in similar studies on other types of clay (Doherty and Gavin 2011; Randolph 2003) which suggests that the increase of total radial stresses with depth intensifies with the preconsolidation pressure of clay layers. Moreover, a comparison between Figs. 4(b) and 6 shows that the variations of radial total stresses resemble

the end resistance changes with depth which implies that σ_{ri} values are controlled by the soil state (Doherty and Gavin 2011), contrary to sandy soils in which variations of σ_{ri} are independent of the soil state (Chow and Jardine 1996).

For a proper understanding of pile behavior and to draw a clearer picture of effective stress conditions, pore pressure values should be provided in addition to radial total stresses. Fig. 7 shows the experimentally measured installation pore pressures and their corresponding numerical predictions obtained through MCC, S-CLAY1 and Creep-SCLAY1S models. Note that in terms of field data the figure only shows the stationary values of pore pressure u_s measured during the installation pause periods (Lehane and Jardine 1994). The figure illustrates that the numerical results fit well with the experimental measurements and predict similar trends. The predictions made by MCC and S-CLAY1S models are approximately equal while the Creep-SCLAY1S model predicts slightly higher pore pressure values. Nevertheless, all three models predict a linear increase in pore pressure as depth increases. Such overall trend can also be seen in the experimental data, except that in the field measurement data, depending on penetration depth, two different patterns of pore pressure increase can be observed. As it is indicated by Doherty and Gavin (2011), for penetration depths less than 2.5m, pore pressure increases rapidly and after this depth its rate reduces. Similar trend is also observed in Fig. 6 for the variations of radial total stress. This similarity could be attributed to friction fatigue (Xu et al. 2006) and as it can be seen in Figs. 6 and 7 SCLAY1S and Creep-SCLAY1S models can capture this effect well, and predict similar trends for the values of radial total stress and pore pressure.

Measurements of pore pressure variations and relaxation of radial total stresses, during equalization and after pile jacking, were two of the main features of the Imperial College pile tests (Doherty and Gavin 2011). These features are expressed through normalized quantities of pore pressure dissipation factor U_d, and relaxation ratio H/H_i, defined as

International Journal of Geomechanics. Submitted January 11, 2016; accepted June 27, 2016; doi:10.1061/ (ASCE)GM.1943-5622.0000774

$$U_d = \frac{u_{max} - u}{u_{max} - u_0} \tag{9}$$

$$\frac{H}{H_i} = \frac{\sigma_r - u_0}{\sigma_{ri} - u_0} \tag{10}$$

where u is the pore pressure after installation and subsequent consolidation, u_0 is the hydrostatic pore water pressure, u_{max} is the maximum pore pressure reached during pile installation, and σ_r is the radial total stress during consolidation. The variations of these two factors, based on field measurements, are shown in Figs. 8(a) and (b), and are compared with their numerical counterparts predicted by MCC, S-CLAY1S and Creep-SCLAY1S models. As field measurement data shows, H/Hi remained constant for the first few minutes and then reduced steadily, reaching an ultimate value of about 0.5 after seven days (Lehane and Jardine 1994). Such reduction would not occur if the soil next to the pile was elastic and isotropic (Sills 1975). This kind of behavior indicates that there is an interaction of a yield zone, developed next to the pile, with the surrounding soil that has not yielded. As Fig. 8(b) shows, in general all three elasto-plastic models are able to capture the reducing trend of H/H_i; however, the MCC model can only provide reasonable prediction of the variations of relaxation ratio for the early stages of pile consolidation, and it overestimates the field data after half a day of consolidation (i.e., after 700 minutes). The S-CLAY1S and Creep-SCLAY1S models, that consider soil anisotropy, provide predictions that are noticeably closer to the field measurement data. Field dissipation curves shown in Fig. 8(a) are based on measurements taken at different soil depths. As this figure shows, the variations of pore pressure dissipation factor generally mirrors H/H_i changes. Based on field data, the typical times for 50% and 85% excess pore pressure dissipation were about 12 hours and 4 days, respectively. It can be seen in the figure that the MCC and Creep-SCLAY1S models provide comparably similar estimations of pore pressure equalization factors which are smaller than S-CLAY1S predictions. During consolidation as pore pressure dissipates, radial effective

stress σ_r' increases towards a final equilibrium value σ_{rc}'. Fig 8(c) shows the comparison between experimental and numerical variations of normalized radial effective stress σ_r'/σ_{rc}' during equalization. Based on field measurements, after about 2 minutes σ_r' values increased rapidly with time, reaching 85% of σ_{rc}' after about 1000 minutes and near equilibrium after about 4 days. The rate of σ_r' equalization exceeded that for pore pressure dissipation, reportedly because the variations of pore pressures and radial stresses were equal during the later stages of equalization (Lehane and Jardine 1994). As it is shown in Fig. 8(c), all three models can capture the increasing trend of σ_r'/σ_{rc}', and their quantitative consistency with field measurements reduces from S-CLAY1S to Creep-SCLAY1S and MCC models. Numerical predictions of the variations of equalized radial effective stresses with depth are shown in Fig. 9 and are compared with field data. This figure illustrates that all models predict σ_{rc}' to increase with depth, which is in agreement with field measurements; however, the most quantitatively comparable results to field data are provided by Creep-SCLAY1S model. As it was indicated by Randolph (2003), the reliability of existing predictive models for accurate evaluation of effective stresses is one of the main concerns regarding application of these models. The comparisons carried out in this section show that Creep-SCLAY1S model provides more accurate and reliable results compared to the other two time-independent models.

Variations of Undrained shear Strength

As the result of pile jacking into the ground, the undrained shear strength c_u of the soil surrounding the pile deviates from its initial value corresponding to the undisturbed soil, c_{u0}. For the soil surrounding the pile, Figs. 10(a) and (b) show the variations of normalized undrained shear strength c_u/c_{u0} predicted by MCC, S-CLAY1S and Creep-SCLAY1S models, both after pile installation and consolidation. Experimental studies show that, right after pile jacking, the installation of displacement piles in soft soil results in the reduction of undrained shear strength

of the soil close to the pile (Serridge and Sarsby 2008). Fig. 10(a) illustrates that while S-CLAY1S and Creep-SCLAY1S predict this reduction, MCC model fails to capture such reduction and instead it predicts that shortly after installation the soil surrounding the pile gains an increased shear strength. The results shown in Fig. 10(a) also suggest that based on anisotropic models predictions the shear strength reductions are more significant for the soil that is within about three radii from the pile surface, and beyond that the decrease in soil's undrained shear strength is more moderate, up to a distance of about 15 radii from the pile surface where shear strength changes are insignificant. As it was discussed by Castro and Karstunen (2010), the large reductions of undrained shear strength close to the pile can be attributed to the loss of soil structure, and the small reductions at further distances are owing to the reduction of effective mean pressure.

After consolidation, the undrained shear strength increases (see Fig. 10(b)). This increase in close vicinity of the pile surface is more noticeable, and further away from the pile surface in areas which are less affected by the pile, this increase is minimal. However, the three constitutive models provide different estimations of this shear strength increase. For instance, close to the cavity wall, MCC model provides predictions which can be up to 90% different from S-CLAY1S and Creep-SCLAY1S models, while beyond fifteen pile radii all three models are quantitatively similar. Fig. 11 shows the variations of undrained shear strength near the cavity wall and during the equalization period. As it can be seen in this figure, S-CLAY1S and Creep-SCLAY1S models predict that the undrained shear strength, right after pile installation, are 50% and 30% less than c_{u0}, while MCC predicts it to be 40% more than c_{u0}. As time elapses and excess pore pressure dissipates, all three models show increasing undrained shear strength due to excess pore pressure dissipation and increase in mean effective stresses. The Creep-SCLAY1S model, in the early stages of consolidation predicts higher undrained shear strength compared to the S-CLAY1S

model; however, its equalized undrained shear strength is smaller because creep causes additional relaxation of radial stresses.

Sensitivity Analysis

Penetration of a pile in a natural soft clay deposit results in destructuration, i.e., degradation of the soil internal structure, which consequently influences the yielding of the soil. In this section the sensitivity of numerical predictions of soil behavior during equalization is investigated against variations of initial anisotropy and bonding (represented by parameters α_0 and χ_0, respectively) which indicate the state of the yield surface inclination and structure of the soil at the onset of the consolidation stage. Fig. 12 shows the S-CLAY1S and Creep-SCLAY1S predictions of radial effective stresses for α_0 values changing ±20% around its representative value. This figure illustrates that the higher the initial anisotropy parameter is, the lower the predicted radial effective stress would be. However, comparing these results with corresponding results in Fig. 9 shows that using α_0 with ±20% different values does not have a significant qualitative and quantitative effect on numerical results. Similar trends can be distinguished in Fig. 13 which depicts the effect of χ_0 variations on numerical predictions of radial effective stresses.

The sensitivity of numerical results, in time domain, to the alteration of initial bonding and anisotropy parameters is shown in Figs. 14 and 15, respectively. As these two figures show, ±20% variation of these parameters does not have considerable effect on numerical predictions. Overall, the sensitivity analyses performed in this section confirms that initial values of anisotropy and bonding parameters have negligible effects on numerical predictions of S-CLAY1S and Creep-SCLAY1S models, and therefore for a reasonably accurate evaluation of the initial values of anisotropy and bonding, these models' performances are reliable.

International Journal of Geomechanics. Submitted January 11, 2016; accepted June 27, 2016; doi:10.1061/ (ASCE)GM.1943-5622.0000774

Installation effect on soil structure

The effect of pile setup on surrounding soil structure can be investigated through the variations of bonding parameter χ which represents the sensitivity of the soil. Fig. 16 shows the S-CLAY1S and Creep-SCLAY1S predictions of normalized bonding parameter, in different distances from pile surface, after installation and soil consolidation phases. The results illustrated in this figure are obtained for different initial bonding parameter values to confirm that χ_0 has no major effect on numerical simulations and hence can be reasonably utilized for normalization of χ. Fig. 16 shows that installation of pile results in the reduction of bonding parameter. This reduction is understandably more intense close to the pile surface. Moreover, the figure also shows that the predictions of both S-CLAY1S and Creep-SCLAY1S models are comparably similar after installation. However, as time passes and the soil consolidates, the results of rate-dependent model deviates from the rate-independent S-CLAY1S model. The comparison between χ/χ_0 after installation and consolidation reveals that there is further reduction of bonding parameter after consolidation. This extra reduction predicted by S-CLAY1S model is smaller than that of Creep-SCLAY1S. Therefore, the Creep-SCLAY1S model predicts the contribution of consolidation process in reduction of χ to be bigger than what it was thought before (discussed in Castro and Karstunen 2010); however, it can still be concluded that the reduction of χ is mainly caused by the undrained cavity expansion.

Installation effect on soil anisotropy

Similar to χ, installation of a pile affects the soil fabric orientation and consequently the inclination of the representative yield surface. Fig. 17 shows the variation of α for different α_0 values after installation of the pile and consolidation of the soil predicted by the advanced anisotropic models. As it can be seen in this figure, after installation and consolidation, the value

of anisotropy parameter in close vicinity of the pile (distances up to 2 pile radii from the surface) is independent of α_0 and both models provide similar predictions of α. In further distances, up to 4 pile radii, while both models provide similar evaluation of α after installation, the Creep-SCLAY1S model predicts lower anisotropy parameter after consolidation. In distances beyond 4 pile radii, the value of α depends on α_0, however the patterns of numerical predictions follow the aforementioned trends. In other words, in this radial distances from the pile both models have comparably similar evaluations of α after installation while S-CLAY1S model predicts higher α values after consolidation. Fig. 17 illustrates that, after installation, the value of α on the pile surface increases when α_0=0.47 and decreases when α_0=0.59 and 0.71. After consolidation, for α_0=0.47 and 0.59, the anisotropy parameter on the pile surface exceeds α_0 while remains smaller than α_0 when α_0=0.71. These trends are sustained in distances less than $1.5r_c$, and beyond that α is less than α_0 and tends toward α_0 at further distances from the pile.

To clarify the trends observed in Fig. 17, variations of radial α_r and axial α_y components of anisotropy tensor are shown in Figs. 18–21. Also to check the sensitivity of these components to the value of initial anisotropy parameter, the variations of α_r and α_y are evaluated for ±20% alteration of α_0 around its representative value and the results are depicted in Figs. 18 and 19. Similar sensitivity analysis is also carried out for the effects of alteration of χ_0 on the variations of α_r and α_y (Figs. 20 and 21). Figs. 18 and 20 suggest that α_r after installation and consolidation reduces as the distance from the surface of the pile increases; and, on the pile surface, α_r after consolidation is higher than that caused by undrained expansion of cavity. In contrary to this trend, Figs. 19 and 21 show that α_y increases as the distance from the pile surface increases. These figures also illustrate that both numerical models provide reasonably comparable results and these results are not sensitive to α_0 and χ_0 values.

International Journal of Geomechanics. Submitted January 11, 2016; accepted June 27, 2016; doi:10.1061/ (ASCE)GM.1943-5622.0000774

Discussion

The comparison of the numerical results in two stages of pile setup history, installation and equalization, reveals that the models which take into account the natural features of the soil behavior, namely anisotropy, destructuration and time effects, provide comparable results during installation period (Figs. 6 and 7). The predictions of SCLAY1S and Creep-SCLAY1S models after installation are in good agreement with the experimental measurements while the MCC model provides less comparable results. In other words, after installation, both SCLAY1S and Creep-SCLAY1S models provide representative and approximately similar predictions of radial effective stresses, pore pressures, and undrained shear strengths (Figs. 6, 7 and 10, respectively). While MCC predictions in some cases (e.g., pore water pressure) are consistent with the two other models, in other cases its simulation results deviate from the measurement data as well as the predictions of the two advanced models. This is mainly due to the fact that pile installation significantly influences the fabric orientation and structure of the surrounding natural soils (Figs. 16 and 17), as well as their yielding characteristics, and these are the aspects of the natural soil behavior that are not taken into account by the MCC model.

Despite undrained expansion of cavity, considerable differences can be distinguished between numerical predictions of SCLAY1S and Creep-SCLAY1S models during equalization period (Figs. 18–21). This can be reasonably expected as the influence of creep increases with time. However, similar comparative studies by Sivasithamparam et al. (2015) showed that even during undrained loading stage, consideration of time-dependency has significant effects on the numerical simulation results, and hence it should be taken into account (particularly when modeling the behavior of soft and sensitive clay). The effects that pile setup has on the variations of soil anisotropy and natural structure, both after installation and consolidation periods, are well-pronounced in Figs. 18–21. From a qualitative standpoint, both models provide predictions which

are consistent with the experimental results. For instance, the experimental measurements indicate that as a result of total stress relaxations during consolidation, the final radial effective stresses become less than their corresponding initial values (Randolph 2003). Both models provide qualitatively similar results while it is the creep model that predicts more quantitatively consistent representation of the field measurements (see Fig. 9).

One of the main advantages of the recently developed Creep-SCLAY1S model is that, unlike the majority of visoplastic models that are based on Perzina's overstress theory (Hinchberger and Rowe 2005; karstunen and Yin 2010), its viscous (i.e., creep) parameters have clear physical meaning and are relatively simple to determine. As indicated earlier in the paper, compared to the MCC the additional parameters of the S-CLAY1 family of models are physically plausible parameters with established procedures for their determination that are well-explained in the literature. This simplicity of parameter determination, and the fact that these advanced models are hierarchical extensions of the widely used MCC model, makes their practical application reasonably straightforward.

Conclusions

Piles are designed to carry loads for a long period of time. During pile installation, the soil around the pile experiences plastic deformations, destructuration, and pore pressure variations. These effects are more pronounced on natural clayey deposits, mainly due to their high sensitivity and low permeability. The consequences of soil alteration are essential on pile capacity; therefore, evaluation of the long term soil modification around the pile is important for proper design and construction of pile foundations, particularly in natural cohesive soils. In the present paper, alteration of a soft clayey soil due to installation of close-ended pile has been numerically investigated. For this purpose, two advanced constitutive models of S-CLAY1 family, which

account for soil anisotropy, destructuration and time effects (in case of the creep model) have been used. Using fully integrated implicit numerical scheme, these models have been implemented as user-defined models in PLAXIS 2D and were employed to investigate the soft soil response to pile setup. The advanced constitutive models provided reliable predictions of soil behavior, variations of pile capacity and soil's structural alteration with time. To highlight the significance of considering natural features of soil behavior in the modeling, corresponding numerical predictions of MCC model have also been provided. The comparison between the predictions of the time-dependent model against field measurements of the case study pile validated the capability of the Creep-SCLAY1S model in qualitatively and quantitatively capturing the observed soil behavior. These comparisons also illustrated the shortcomings of classical MCC model and supported the impact of considering soil natural features for a reasonably accurate and reliable numerical modeling work. The series of sensitivity analyses that has been carried out showed that the variations of initial values of yield surface inclination and bonding parameters have almost negligible effects on numerical predictions. Furthermore, these analyses showed that, while time-independent and time-dependent S-CLAY1-based models provide reasonably comparable results of the soil behavior after pile setup, consideration of time effects better represent the changes in radial effective stresses (known as the underlying mechanism of pile installation effects for displacement piles in soft clays) that occur during installation and subsequent dissipation of excess pore pressures.

References

Albert, C., Zdravkovic, L., and Jardine, R. (2003). "Behaviour of Bothkennar clay under rotation of principal stresses." *Proceedings of the International Workshop on Geotechnics of Soft Soils-Theory and Practice.* Essen, Germany, 441-447.

Augustesen, A., Andersen, L., and Sørensen, C. S. (2006). "Assessment of time functions for piles driven in clay." *DCE Technical Memorandum*, Department of Civil Engineering, Aalborg University.

Azzouz, A., and Morrison, M. (1988). "Field measurements on model pile in two clay deposits." *Journal of Geotechnical Engineering*, 114(1), 104-121.

Bond, A. J., Dalton, J., and Jardine, R. J. (1991). "Design and performance of the Imperial College instrumented pile." *ASTM Geotechnical Testing Journal*, 14(4), 413-424.

Bond, A. J., and Jardine, R. J. (1991). "Effects of installing displacement piles in a high OCR clay." *Géotechnique*, 41(3), 341-363.

Brinkgreve, R. B. J., Swolfs, W. M., and Engin, E. (2013). "PLAXIS 2D anniversary edition reference manual." Delft University of Technology and PLAXIS, The Netherlands.

Burns, S., and Mayne, P. (1999). "Pore pressure dissipation behavior surrounding driven piles and cone penetrometers." *Transportation Research Record: Journal of the Transportation Research Board*, 1675, 17-23.

Carter, J. P., Randolph, M. F., and Wroth, C. P. (1979). "Stress and pore pressure changes in clay during and after the expansion of a cylindrical cavity." *International Journal for Numerical and Analytical Methods in Geomechanics* 3(4), 305-322.

Castro, J., and Karstunen, M. (2010). "Numerical simulations of stone column installation." *Canadian Geotechnical Journal*, 47(10), 1127-1138.

Castro, J., Karstunen, M., Sivasithamparam, N., and Sagaseta, C. (2013)."Numerical analyses of stone column installation in Bothkennar clay." *Proceedings of the International*

Conference on Installation Effects in Geotechnical Engineering, Rotterdam, The Netherlands, 212-218.

Chow, F., and Jardine, R. J. (1996). "Investigations into the behaviour of displacement piles for offshore foundations." *International Journal of Rock Mechanics and Mining Sciences and Geomechanics Abstracts*, 33(7), 319A-320A.

Clausen, C. J. F., and Aas, P. M. (2000). "Bearing capacity of driven piles in clays." *NGI report* Norwegian Geotechnical Institute.

Collins, I. F., and Stimpson, J. R. (1994). "Similarity solutions for drained a undrained cavity expansions in soils." *Géotechnique*, 44(1), 21-34.

Dafalias, Y. F. (1987). "An anisotropic critical state clay plasticity model." *Proceedings of the 2nd International Conference on Constitutive Laws for Engineering Materials.* Tucson, US, 513-521.

Dafalias, Y. F., Manzari, M. T., and Papadimitriou, A. G. (2006). "SANICLAY: simple anisotropic clay plasticity model." *International Journal for Numerical and Analytical Methods in Geomechanics* 30(12), 1231-1257.

Davies, M., and Newson, T. (1993). "A critical state constitutive model for anisotropic soil." *Predictive Soil Mechanics, Proceedings of the Wroth Memorial Symposium*, Thomas Telford, London, 219–229.

Doherty, P., and Gavin, K. (2011). "The shaft capacity of displacement piles in clay: A state of the art review." *Geotechnical and Geological Engineering* 29(4), 389-410.

Doherty, P., and Gavin, K. (2011). "Shaft capacity of open-ended piles in clay." *Journal of Geotechnical and Geoenvironmental Engineering*, 137(11), 1090-1102.

Fellenius, B., Riker, R., O'Brien, A., and Tracy, G. (1989). "Dynamic and static testing in soil exhibiting set-up." *Journal of Geotechnical Engineering*, 115(7), 984-1001.

Gallagher, D., Gavin, K., McCabe, B., and Lehane, B. (2004). "Experimental investigation of the response of a driven pile in soft silt." *Proceedings of the 18th Australasian Conference on the Mechanics of Structures and Materials*, Perth, Australia, Vol. II, 991-996.

Gens, A., and Nova, R. (1993). "Conceptual bases for a constitutive model for bonded soils and weak rocks." *Geotechnical engineering of hard soils-soft rocks*, 1(1), 485-494.

Graham, J., Noonan, M. L., and Lew, K. V. (1983). "Yield states and stress–strain relationships in a natural plastic clay." *Canadian Geotechnical Journal*, 20(3), 502-516.

Grimstad, G., Degago, S., Nordal, S., and Karstunen, M. (2010). "Modeling creep and rate effects in structured anisotropic soft clays." *Acta Geotechnica* 5(1), 69-81.

Gwizdała, K., and Więcławski, P. (2013). "Influence of time on the bearing capacity of precast piles." *Studia Geotechnica et Mechanica*, 35(4), 65-74.

Heydinger, A. G., and O'Neill, M. W. (1986). "Analysis of axial pile-soil interaction in clay." *International Journal for Numerical and Analytical Methods in Geomechanics* 10(4), 367-381.

Hinchberger, S. D., and Rowe, R. K. (2005). "Evaluation of the predictive ability of two elastic-viscoplastic constitutive models." *Canadian Geotechnical Journal*, 42(6), 1675-1694.

Holtz, W. G., and Lowitz, C. A. (1965). "Effects of driving displacement piles in lean clay." *Journal of the Soil Mechanics and Foundations Division*, 91(5), 1-14.

Houlsby, G. T., Kelly, R. B., Huxtable, J., and Byrne, B. W. (2005). "Field trials of suction caissons in clay for offshore wind turbine foundations." *Géotechnique*, 55(4), 287-296.

Karstunen, M., Krenn, H., Wheeler, S., Koskinen, M., and Zentar, R. (2005). "Effect of anisotropy and destructuration on the behavior of Murro Test embankment." *International Journal of Geomechanics* 5(2), 87-97.

Karstunen, M., Wiltafsky, C., Krenn, H., Scharinger, F., and Schweiger, H. F. (2006). "Modelling the behaviour of an embankment on soft clay with different constitutive models." *International Journal for Numerical and Analytical Methods in Geomechanics* 30(10), 953-982.

karstunen, M., and Yin, Z.-Y. (2010). "Modelling time-dependent behaviour of Murro test embankment." *Géotechnique*, 60(10), 735-749.

Kavvadas, M. (1982). "Non-linear consolidation around driven piles in clays." PhD, Massachusetts Institute of Technology.

Kim, D. (2004). "Comparisons of constitutive models for anisotropic soils." *KSCE Journal of Civil Engineering*, 8(4), 403-409.

Kirsch, F. (2006). "Vibro stone column installation and its effect on ground improvement." *Proceedings of the International Conference on Numerical Modelling of Construction Processes in Geotechnical Engineering for Urban Environment,* Bochum, Germany, 115-124.

Konrad, J.-M., and Roy, M. (1987). "Bearing capacity of friction piles in marine clay." *Géotechnique*, 37(2), 163-175.

Lehane, B. M., and Jardine, R. J. (1994). "Displacement-pile behaviour in a soft marine clay." *Canadian Geotechnical Journal*, 31(2), 181-191.

Leoni, M., Karstunen, M., and Vermeer, P. A. (2008). "Anisotropic creep model for soft soils." *Géotechnique*, 58(3), 215-226.

Liyanapathirana, D. (2008). "A numerical model for predicting pile setup in clay." *Proceedings of GeoCongress 2008: Characterization, Monitoring, and Modeling of GeoSystems*, American Society of Civil Engineers, USA, 710-717.

McGinty, K. (2006). "The stress-strain behaviour of Bothkennar clay." PhD, University of Glasgow.

Niarchos, D. G. (2012). "Analysis of consolidation around driven piles in overconsolidated clay." MSc, Massachusetts Institute of Technology.

Nishimura, S., Minh, N. A., and Jardine, R. J. (2007). "Shear strength anisotropy of natural London Clay." *Géotechnique*, 57(1), 49-62.

O'Neill, M. W., Hawkins, R. A., and Audibert, J. M. (1982). "Installation of pile group in overconsolidated clay." *Journal of the Geotechnical Engineering Division*, 108(11), 1369-1386.

Pestana, J., Hunt, C., and Bray, J. (2002). "Soil deformation and excess pore pressure field around a closed-ended pile." *Journal of Geotechnical and Geoenvironmental Engineering*, 128(1), 1-12.

Randolph, M. F. (2003). "Science and empiricism in pile foundation design." *Géotechnique*, 53(10), 847-875.

Randolph, M. F., Carter, J. P., and Wroth, C. P. (1979). "Driven piles in clay: the effects of installation and subsequent consolidation." *Géotechnique*, 29(4), 361-393.

Roscoe, K. H., and Burland, J. (1968). "On the generalized stress-strain behaviour of wet clay." *Engineering Plasticity*, 553-609.

Roy, M., Blanchet, R., Tavenas, F., and Rochelle, P. L. (1981). "Behaviour of a sensitive clay during pile driving." *Canadian Geotechnical Journal*, 18(1), 67-85.

Sekiguchi, H., and Ohta, H. (1977). "Induced anisotoropy and time dependency in clay." *Proceedings of the 9th ICSMFE, Tokyo, Constitutive Equations of Soils*, 17, 229-238.

Serridge, C. J., and Sarsby, R. W. (2008). "A review of field trials investigating the performance of partial depth vibro stone columns in a deep soft clay deposit." *Geotechnics of Soft Soils: Focus on Ground Improvement*, Taylor & Francis, 293-298.

Sheil, B. B., McCabe, B. A., Hunt, C. E., and Pestana, J. M. (2015). "A practical approach for the consideration of single pile and pile group installation effects in clay: Numerical modelling." *Journal of Geo-Engineering Sciences*, 2(3, 4), 119-142.

Sills, G. C. (1975). "Some conditions under which Biot's equations of consolidation reduce to Terzaghi's equation." *Géotechnique*, 25(1), 129-132.

Sivasithamparam, N. (2012). "Development and implementation of advanced soft soil models in finite elements." PhD, University of Strathclyde.

Sivasithamparam, N., Karstunen, M., and Bonnier, P. (2015). "Modelling creep behaviour of anisotropic soft soils." *Computers and Geotechnics*, 69, 46-57.

Soderberg, L. O. (1962). "Consolidation theory applied to foundation pile time effects." *Géotechnique*, 12(3), 217-225.

Svinkin, M. R., Morgano, C. M., and Morvant, M. (1994). "Pile capacity as a function of time in clayey and sandy soils." *Proceedings of the 5th International Conference and Exhibition on Piling and Deep Foundations*, 1.11.1–1.11.8.

Vermeer, P. A., Stolle, D. F. E., and Bonnier, P. G. (1998). "From the classical theory of secondary compression to modern creep analysis." *Proceedings of the Computer Methods and advances in Geomechanics*, Balkema, Rotterdam, Netherlands, 2469-2478.

Wheeler, S., Karstunen, M., and Naatanen, A. (1999). "Anisotropic hardening model for normally consolidated soft, clays." *Proceedings of the 7th International Symposium on Numerical Models in Geomechanics*, Balkema, Rotterdam, The Netherlands, Vol. II , 33–40.

Wheeler, S. J., Näätänen, A., Karstunen, M., and Lojander, M. (2003). "An anisotropic elastoplastic model for soft clays." *Canadian Geotechnical Journal*, 40(2), 403-418.

Whittle, A., and Kavvadas, M. (1994). "Formulation of MIT-E3 Constitutive Model for Overconsolidated Clays." *Journal of Geotechnical Engineering*, 120(1), 173-198.

Xu, X. T., Liu, H. L., and Lehane, B. M. (2006). "Pipe pile installation effects in soft clay." *Proceedings of the Institution of Civil Engineers - Geotechnical Engineering*, 159(4), 285-296.

Yildiz, A. (2009). "Numerical modeling of vertical drains with advanced constitutive models." *Computers and Geotechnics*, 36(6), 1072-1083.

Yu, H.-S. (1990). "Cavity expansion theory and its application to the analysis of pressuremeters." PhD, University of Oxford.

Yu, H.-S. (2000). *Cavity expansion methods in geomechanics*, Springer.

Zhou, C., Yin, J., Zhu, J., and Cheng, C. (2005). "Elastic Anisotropic Viscoplastic Modeling of the Strain-Rate-Dependent Stress–Strain Behavior of K0 -Consolidated Natural Marine Clays in Triaxial Shear Tests." *International Journal of Geomechanics* 5(3), 218-232.

Zwanenburg, C. (2013). "Application of SCLAY1 model to peat mechanics." Internal Report, Deltares, The Netherlands.

International Journal of Geomechanics. Submitted January 11, 2016; accepted June 27, 2016; doi:10.1061/ (ASCE)GM.1943-5622.0000774

Figure Captions:

Fig. 1 Yield surfaces of the S-CLAY1S model in a) general stress space, and b) triaxial stress space (CSL, critical state line).

Fig. 2 Schematic of the current state surface (CSS) and normal consolidation surface (NCS) of the Creep-SCLAY1 model (in triaxial stress space).

Fig. 3 Configuration of the Imperial College test piles (Lehane and Jardine 1994).

Fig. 4 Variations of a) OCR with depth obtained from oedometer tests, and b) end resistance q_c and pore pressure u_c with depth obtained from *in-situ* piezocone tests (data from Lehane and Jardine 1994).

Fig. 5 Geometry of the boundary value problem and the idealised soil profile.

Fig. 6 Comparison between measured and predicted values of radial total stress σ_{ri}, after pile installation (σ_{h0} is the initial undisturbed horizontal stress) (data from Lehane and Jardine 1994).

Fig. 7 Comparison between measured and predicted values of pore pressure u_s, after pile installation (data from Lehane and Jardine 1994).

Fig. 8 Comparison between measured and predicted values of a) pore pressure; b) radial total stress; c) radial effective stress, during equalization (data from Lehane and Jardine 1994).

Fig. 9 Comparison between measured and predicted values of radial effective stress after equalization (data from Lehane and Jardine 1994).

Fig. 10 Simulation results for variations of undrained shear strength due to pile jacking a) after installation, and b) after equalization.

Fig. 11 Simulation results for relative variations of undrained shear strength with time.

Fig. 12 Effect of anisotropy parameter alterations on radial effective stress predictions after equalization (data from Lehane and Jardine 1994).

Fig. 13 Effect of destructuration parameter alterations on radial effective stress predictions after equalization (data from Lehane and Jardine 1994).

Fig. 14 Effect of anisotropy parameter alterations on variations of radial effective stress during equalization (data from Lehane and Jardine 1994).

Fig. 15 Effect of destructuration parameter alterations on variations of radial effective stress during equalization (data from Lehane and Jardine 1994).

Fig. 16 Simulation results for relative variations of destructuration parameter due to pile setup.

Fig. 17 Simulation results for relative variations of α_0 due to pile setup.

Fig. 18 Changes of α_r due to pile setup with different initial anisotropy values.

Fig. 19 Changes of α_y due to pile setup with different initial anisotropy values.

Fig. 20 Changes of α_r due to pile setup with different initial bonding values.

Fig. 21 Changes of α_y due to pile setup with different initial bonding values.

International Journal of Geomechanics. Submitted January 11, 2016; accepted June 27, 2016; doi:10.1061/ (ASCE)GM.1943-5622.0000774

Table 1. Model parameter values for Bothkennar clay.

Basic parameters								Anisotropy			Structure			
$\gamma\ (kN/m^{-3})$	e_0	OCR	K_0	κ	v'	λ	M	α_0	ω	ω_d	χ_0	λ_i	ξ	ξ_d
16.5	2	1.5	0.5	0.02	0.2	0.3	1.5	0.59	50	1	8	0.18	9	0.2

Table 2. Additional creep parameter values for Bothkennar clay.

μ^*	μ_i^*	τ (days)
5.07×10^{-3}	2×10^{-3}	1

Table 3. Permeability values for Bothkennar clay deposit.

Depth (m)	k_h(m/day)	k_v(m/day)
0-1	2.42×10^{-4}	1.21×10^{-4}
1-6	1.21×10^{-4}	5.96×10^{-5}

Figure 1.pdf

International Journal of Geomechanics. Submitted January 11, 2016; accepted June 27, 2016; doi:10.1061/ (ASCE)GM.1943-5622.0000774

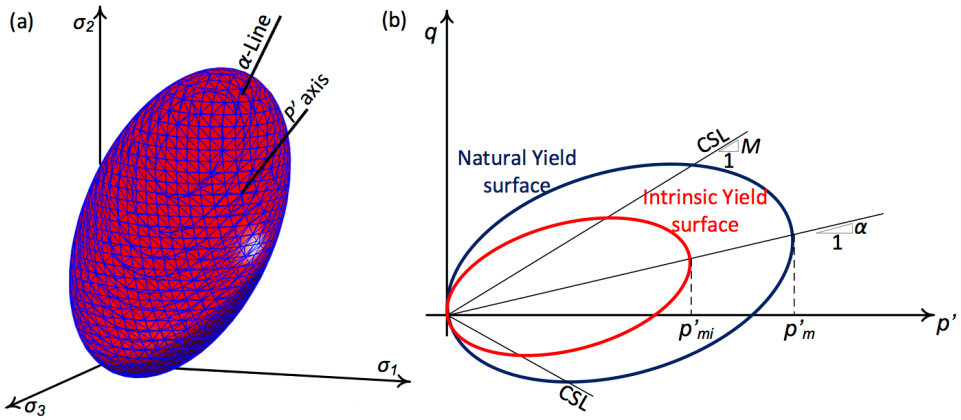

Figure 2.pdf

International Journal of Geomechanics. Submitted January 11, 2016; accepted June 27, 2016; doi:10.1061/ (ASCE)GM.1943-5622.0000774

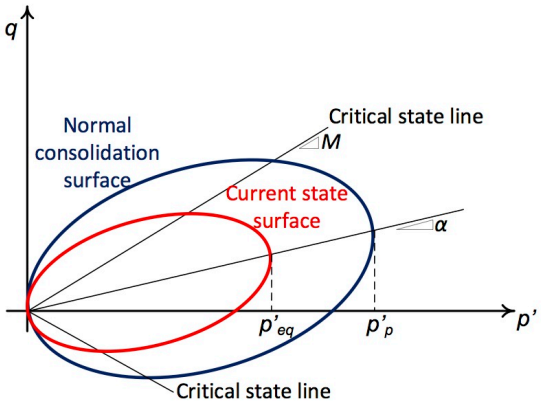

Figure 3.pdf

International Journal of Geomechanics. Submitted January 11, 2016; accepted June 27, 2016; doi:10.1061/ (ASCE)GM.1943-5622.0000774

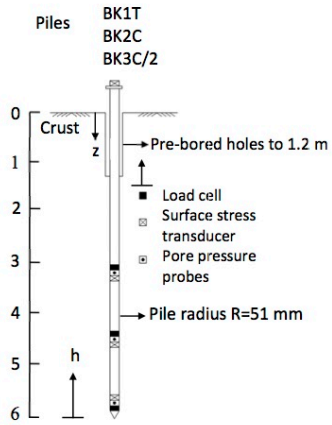

International Journal of Geomechanics. Submitted January 11, 2016; accepted June 27, 2016; doi:10.1061/ (ASCE)GM.1943-5622.0000774

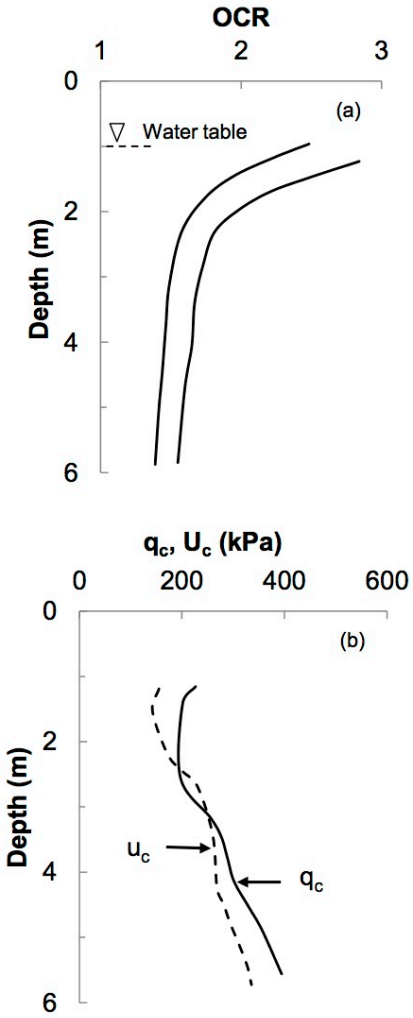

Figure 5.pdf

International Journal of Geomechanics. Submitted January 11, 2016; accepted June 27, 2016; doi:10.1061/ (ASCE)GM.1943-5622.0000774

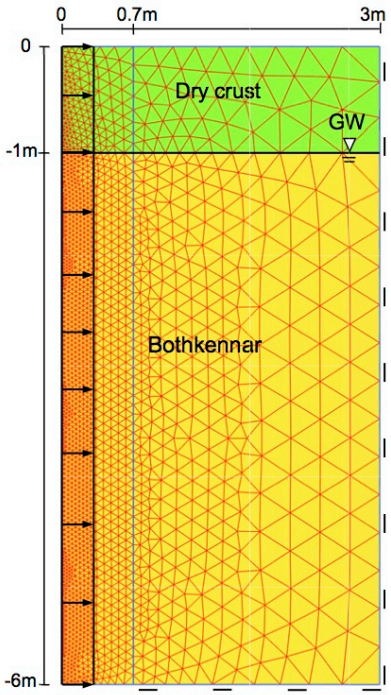

Figure 6.pdf

International Journal of Geomechanics. Submitted January 11, 2016; accepted June 27, 2016; doi:10.1061/ (ASCE)GM.1943-5622.0000774

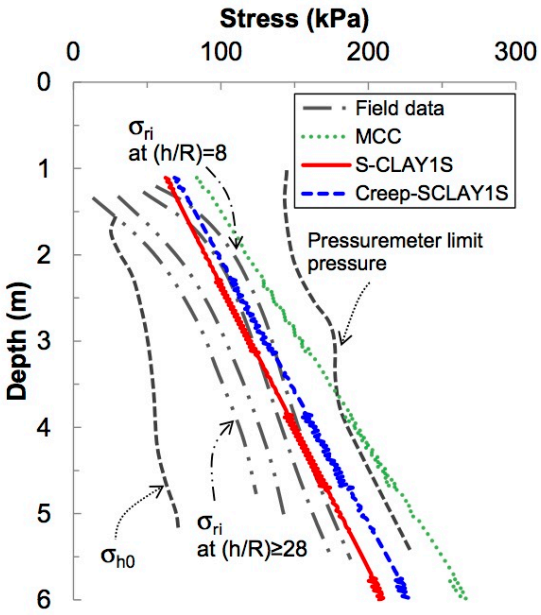

Figure 7.pdf

International Journal of Geomechanics. Submitted January 11, 2016; accepted June 27, 2016; doi:10.1061/ (ASCE)GM.1943-5622.0000774

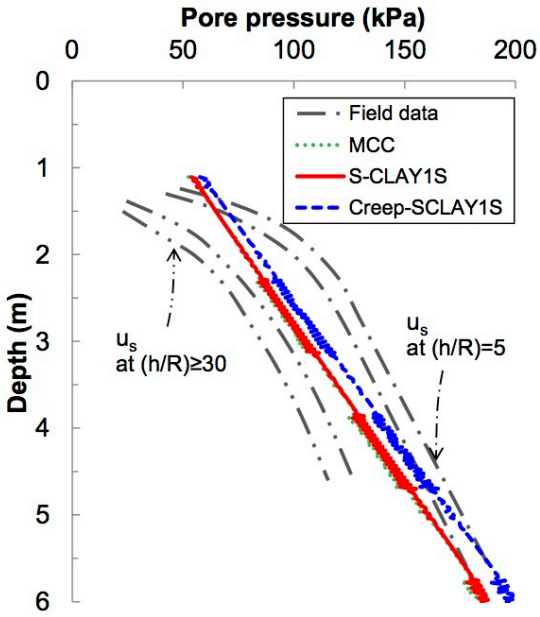

International Journal of Geomechanics. Submitted January 11, 2016; accepted June 27, 2016; doi:10.1061/ (ASCE)GM.1943-5622.0000774

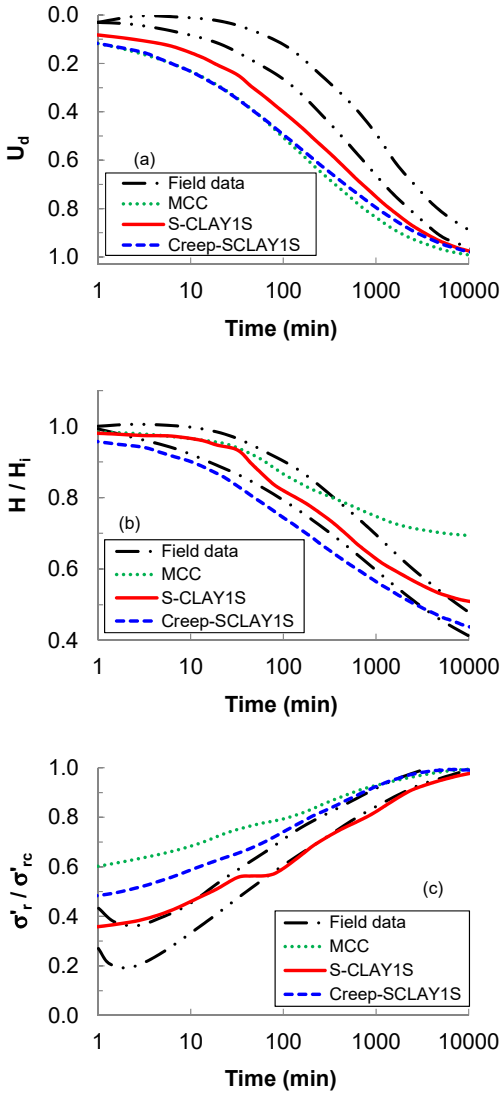

International Journal of Geomechanics. Submitted January 11, 2016; accepted June 27, 2016; doi:10.1061/ (ASCE)GM.1943-5622.0000774

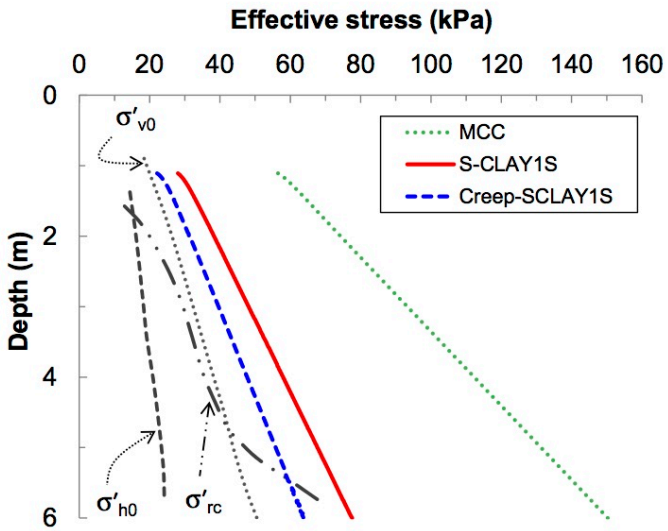

International Journal of Geomechanics. Submitted January 11, 2016; accepted June 27, 2016; doi:10.1061/ (ASCE)GM.1943-5622.0000774

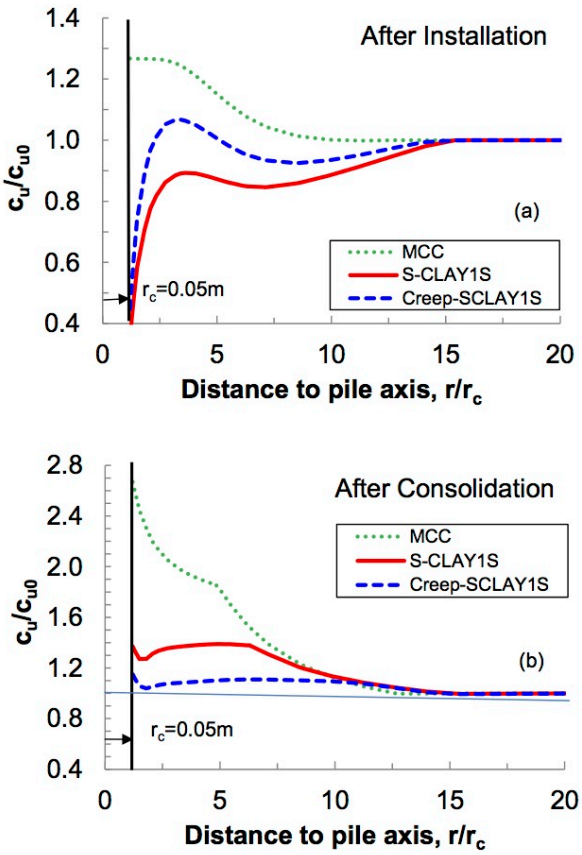

Figure 11.pdf

International Journal of Geomechanics. Submitted January 11, 2016; accepted June 27, 2016; doi:10.1061/ (ASCE)GM.1943-5622.0000774

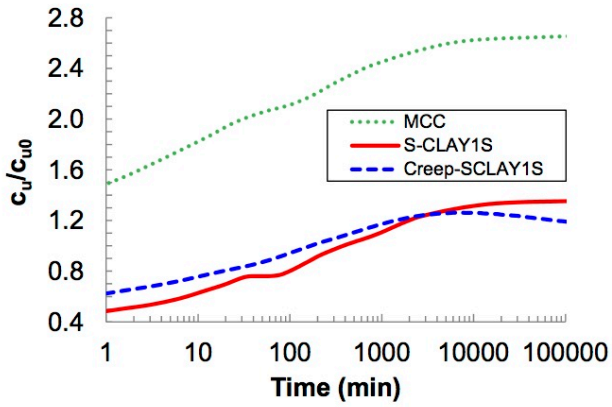

Figure 12.pdf

International Journal of Geomechanics. Submitted January 11, 2016; accepted June 27, 2016; doi:10.1061/ (ASCE)GM.1943-5622.0000774

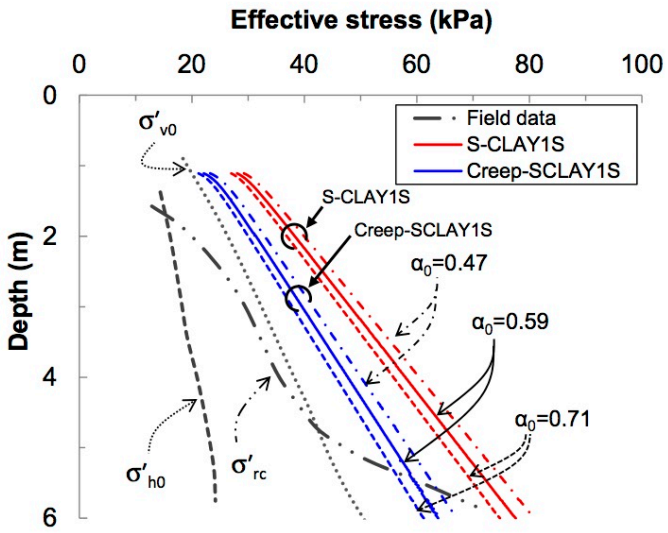

Figure 13.pdf

International Journal of Geomechanics. Submitted January 11, 2016; accepted June 27, 2016; doi:10.1061/ (ASCE)GM.1943-5622.0000774

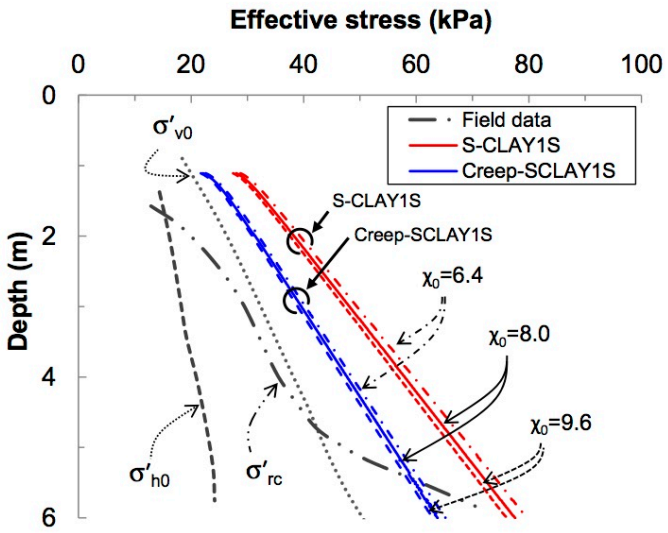

Figure 14.pdf

International Journal of Geomechanics. Submitted January 11, 2016; accepted June 27, 2016; doi:10.1061/ (ASCE)GM.1943-5622.0000774

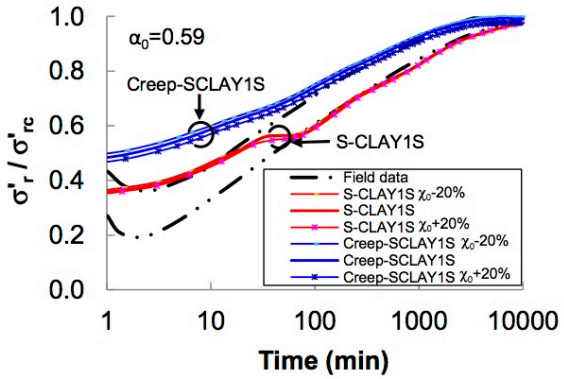

Figure 15.pdf

International Journal of Geomechanics. Submitted January 11, 2016; accepted June 27, 2016; doi:10.1061/ (ASCE)GM.1943-5622.0000774

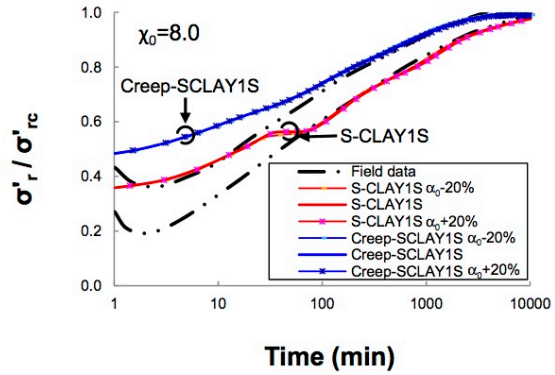

International Journal of Geomechanics. Submitted January 11, 2016; accepted June 27, 2016; doi:10.1061/ (ASCE)GM.1943-5622.0000774

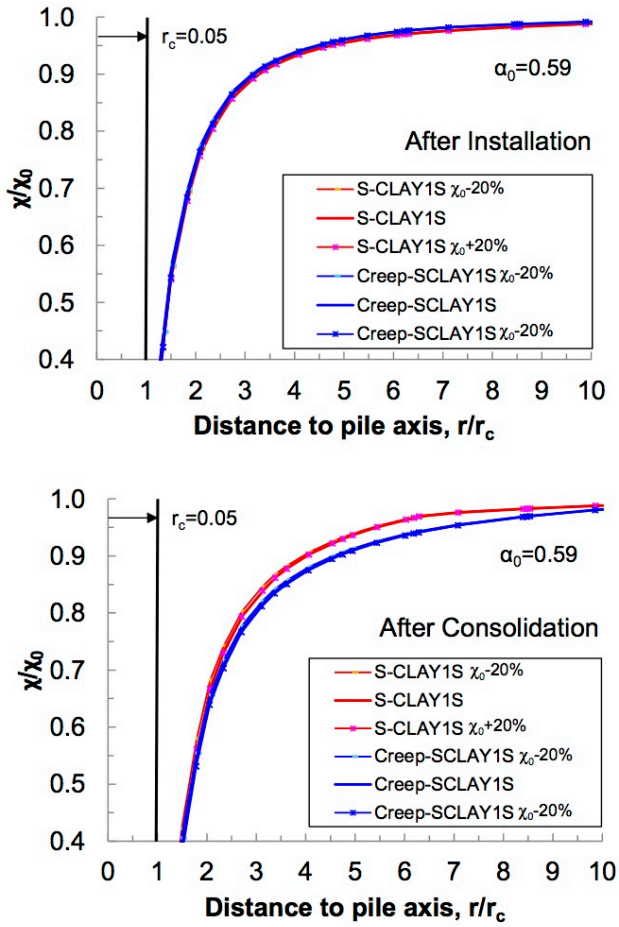

International Journal of Geomechanics. Submitted January 11, 2016; accepted June 27, 2016; doi:10.1061/ (ASCE)GM.1943-5622.0000774

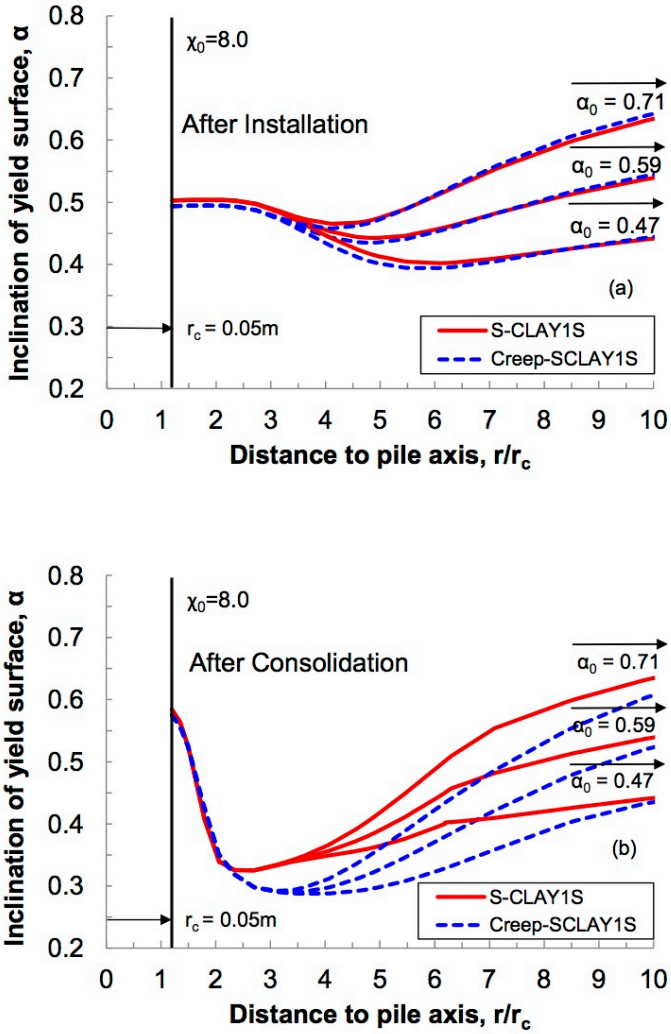

Figure 18.pdf

International Journal of Geomechanics. Submitted January 11, 2016; accepted June 27, 2016; doi:10.1061/ (ASCE)GM.1943-5622.0000774

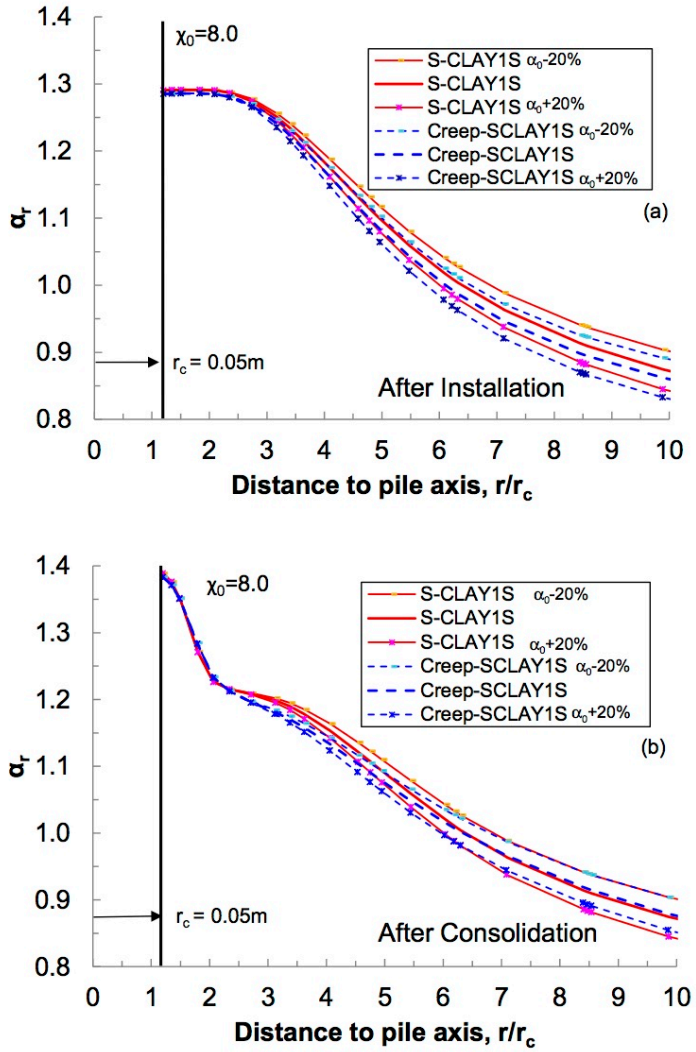

International Journal of Geomechanics. Submitted January 11, 2016; accepted June 27, 2016; doi:10.1061/ (ASCE)GM.1943-5622.0000774

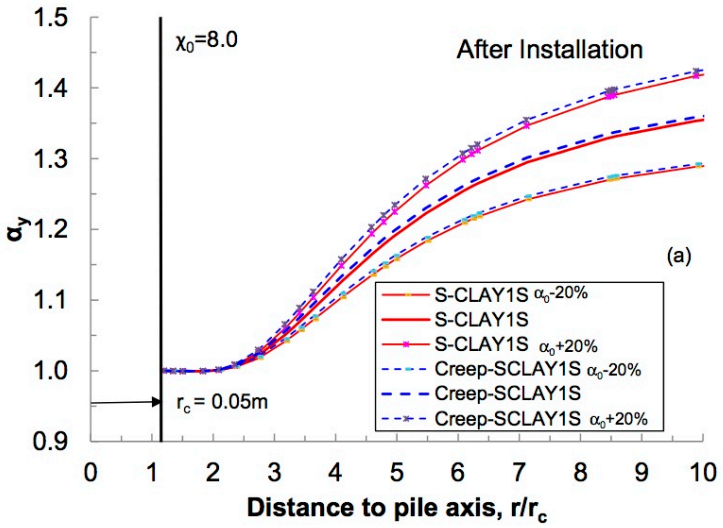

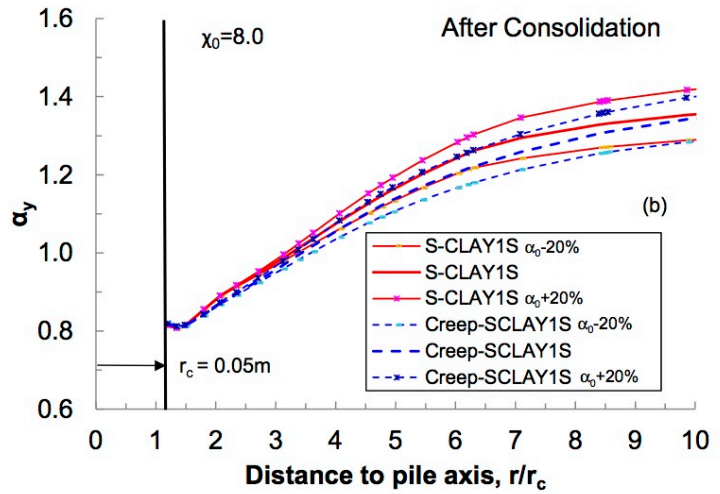

International Journal of Geomechanics. Submitted January 11, 2016; accepted June 27, 2016; doi:10.1061/ (ASCE)GM.1943-5622.0000774

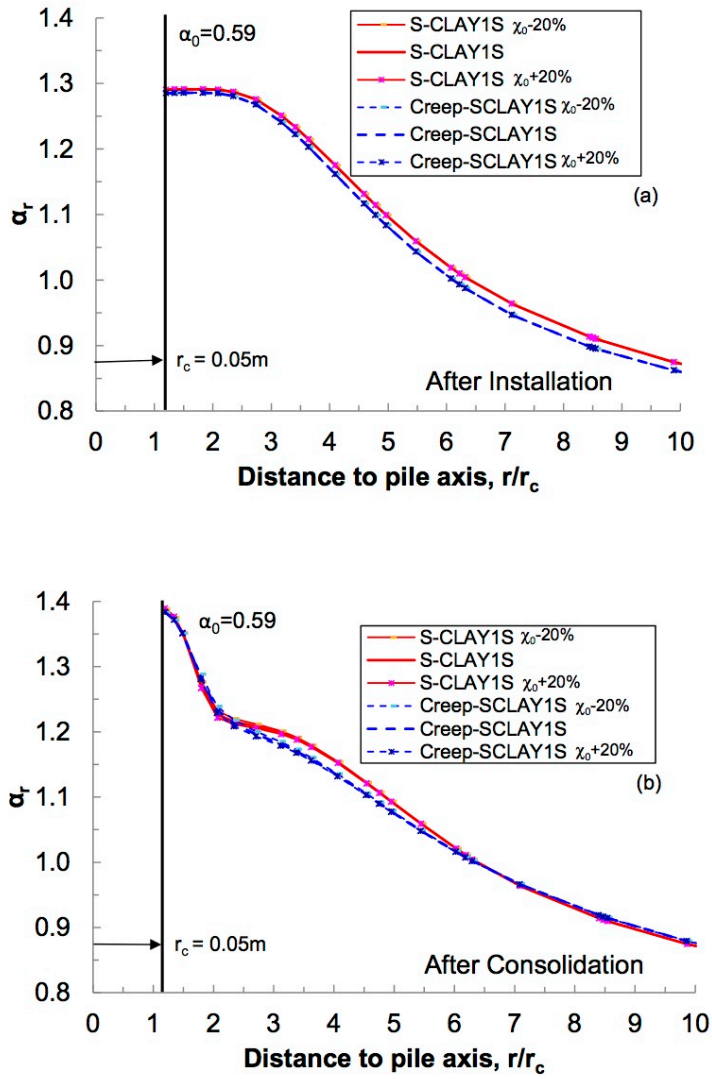

International Journal of Geomechanics. Submitted January 11, 2016; accepted June 27, 2016; doi:10.1061/ (ASCE)GM.1943-5622.0000774